Journal of Inclusion Phenomena and Molecular Recognition in Chemistry **12**: 237–251, 1992.

Molecular Dynamics and the Structure of Macrocycles – Solvent Acetonitrile Interactions

MEIZHEN XU and SERGIO PETRUCCI*
Weber Research Institute and Dept. of Chemistry, Polytechnic University, Long Island Center, Route 110, Farmingdale, NY 11735, U.S.A.

EDWARD M. EYRING*
Department of Chemistry, University of Utah, Salt Lake City, UT 84112, U.S.A.

(Received: 6 September 1990; in final form: 30 January 1991)

Abstract. Microwave complex permittivities, $\varepsilon^* = \varepsilon' - J\varepsilon''$, are reported in the 1–90 GHz frequency range for the macrocycles 18-crown-6 (18C6) and 15C5 added to acetonitrile in stoichiometric proportions, in the solvent CCl_4 at 25°C. Digitized infrared spectra of the 'CN stretch' ν_2 vibration of acetonitrile for the same systems are reported in the 2300–2200 cm^{-1} spectral region. The macrocycle 12C4 added to CH_3CN has also been investigated in the infrared. Both the dielectric relaxation and infrared results are interpreted in terms of macrocycle–acetonitrile interactions, probably involving a methyl-hydrogen to ethereal-oxygen interaction. These interactions with CH_3CN diminish in strength according to the sequence: 18C6 > 15C5 > 12C4.

Key words. Crown ethers, solvent-macrocycle interactions, microwave dielectric relaxation.

1. Introduction

The literature on macrocyclic ligands in solution [1, 2] abounds with information on their most salient interaction, the complexation of metal cations. The isomeric dynamics of macrocycles in aqueous and non-aqueous solvents have also been summarized for simple macrocycles [3]. These previous results focus on the macrocycle itself and on its dynamics in various solvents with the solvent present in excess. Hence, interactive changes of the macrocycles are masked by the more abundant solvent molecules.

In a pioneering effort, mainly utilizing NMR techniques, Mosier-Boss and Popov [4] focused on these macrocycle–solvent interactions by looking at the 18C6–acetonitrile system in 1 : 1 stoichiometric proportions, dissolved in the essentially inert solvent CCl_4. These interactions were expressed quantitatively by formation constants extracted [4] from the NMR data, and the existence of these interactions was confirmed by infrared data.

In the present work, microwave dielectric relaxation techniques were used to probe the effect of mixing the macrocycles (18C6 and 15C5) with acetonitrile (CH_3CN) in the solvent CCl_4 on the molecular relaxation dynamics of both the

This paper is dedicated to the memory of the late Dr C. J. Pedersen.
* Authors for correspondence

macrocycle and CH_3CN. Infrared data on the 'CN stretch' ν_2 vibration proved to be important for the characterization of these interactions.

It will be shown that interaction between CH_3CN and crown ethers diminish in strength in the order 18C6 > 15C5 > 12C4.

2. Experimental

The microwave dielectric instrumentation, the computer assisted infrared spectrometer, and the associated procedures have all been described before [5, 6]. 18C6 (Aldrich) was recrystallized from distilled, dry acetonitrile and dried *in vacuo*. 15C5 and 12C4 (Aldrich) were exposed to molecular sieves for several weeks before use. Acetonitrile (Aldrich, gold label) was refluxed for several hours over P_2O_5 before distilling in an all Pyrex distillation apparatus with no grease on the joints. CCl_4 was also distilled over P_2O_5 in an all Pyrex column.

3. Results and Discussion

3.1. MICROWAVE DIELECTRIC RELAXATION

Figure 1 reports the real part ε' and the loss coefficient ε'' of the complex dielectric permittivity $\varepsilon^* = \varepsilon' - J\varepsilon''$, in the frequency range 1–90 GHz. The system illustrated is the mixture CH_3CN 0.4M + 18C6 0.10M, in the solvent CCl_4 at 25°C. The spectrum profile can be interpreted by two Debye single relaxation dielectric processes, centered at $f_1 = 5$ GHz and $f_2 = 35$ GHz, respectively. Figure 2 reports ε' and the loss coefficient ε'' for CH_3CN 0.4M in CCl_4 at 25°C. The data can be interpreted, within experimental error, by a single Debye relaxation centered at $f_r = 30$ GHz with relaxation parameters comparable to those used for the higher frequency relaxation process of the mixture above. The data for the mixture are expressible by the function

$$\varepsilon = \Delta\varepsilon'_1 \frac{1}{1+(f/f_1)^2} + \Delta\varepsilon'_2 \frac{1}{1+(f/f_2)^2} + \varepsilon_{\infty 2}$$
$$\varepsilon'' = \Delta\varepsilon''_1 \frac{f/f_1}{1+(f/f_1)^2} + \Delta\varepsilon''_2 \frac{f/f_2}{1+(f/f_2)^2} \tag{1}$$

with $\Delta\varepsilon'_1 = \Delta\varepsilon''_1 = \varepsilon_0 - \varepsilon_{\infty 1}$ and $\Delta\varepsilon'_2 = \Delta\varepsilon''_2 = \varepsilon_{\infty 1} - \varepsilon_{\infty 2}$ where ε_0 is the static permittivity, and $\varepsilon_{\infty 1}$ and $\varepsilon_{\infty 2}$ are the permittivity values for frequencies $f > f_1, f_2$.

It is important at this point to compare the results of the macrocycle + CH_3CN in CCl_4 with those of the macrocycle alone in CCl_4 and of CH_3CN alone in CCl_4. The attribution of the relaxation profile of the mixture CH_3CN 0.4M + 18C6 0.1M to two individual Debye processes, with the one at f_2 due to acetonitrile, is strengthened by the results of Figure 1C reporting the microwave dielectric relaxation parameter ε'' of 18C6 0.1M alone in CCl_4 and showing relaxation parameters comparable to those of the lower frequency relaxation component of Figure 3A. In Figure 3A the coefficient of the imaginary part ε'' of ε^* for the mixture CH_3CN 0.1M + 18C6 0.1M in CCl_4 is reported as a function of the frequency f. Figure 3B reports the dielectric spectrum of CH_3CN 0.1M in CCl_4 with parameters again comparable to those of the higher frequency relaxation in Figure 3A.

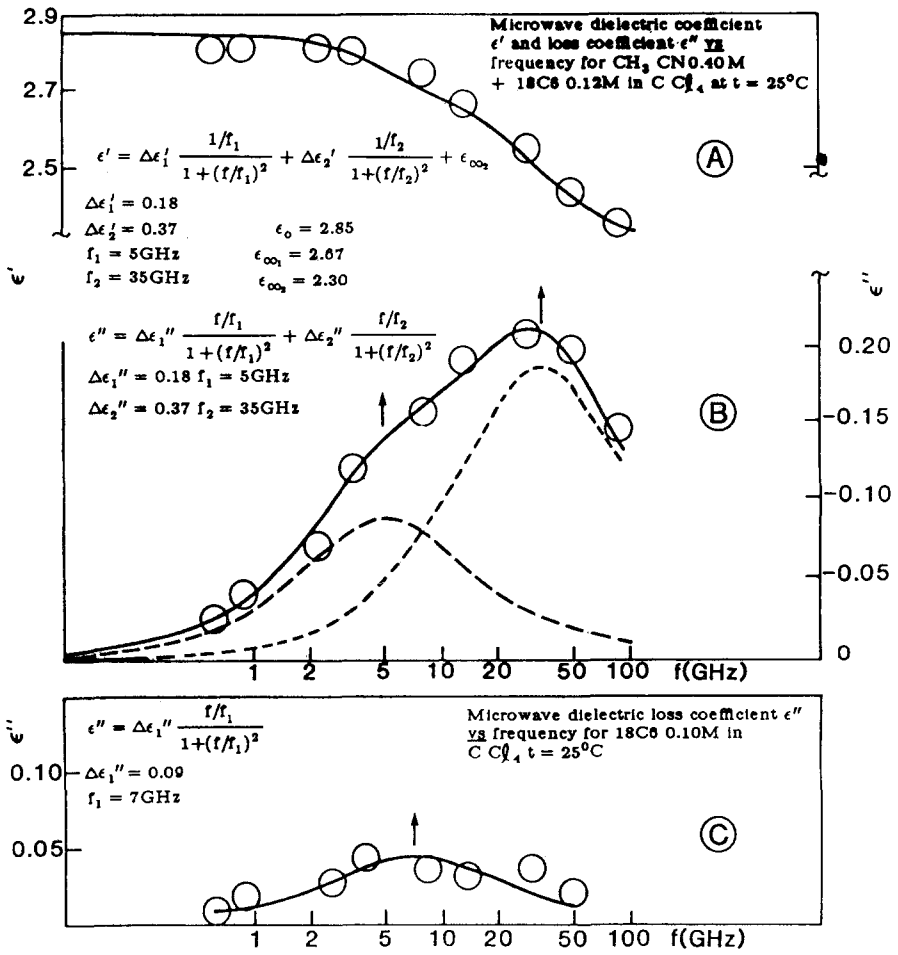

Fig. 1. (A) Microwave dielectric real coefficient ε' of the complex permittivity ε^* vs. frequency f for the mixture CH_3CN 0.4M + 18C6 0.12M in CCl_4 at 25°C. (B) Coefficient of the imaginary part ε'' of the complex permittivity ε^* vs. frequency f for the mixture CH_3CN 0.4M + 18C6 0.12M in CCl_4 at 25°C. (C) ε'' vs. f for 18C6 0.1M in CCl_4 at 25°C.

The relevant issue is that an interpretation of the spectral profile of the mixtures in terms of two relaxation processes, one due to CH_3CN and the other to 18C6, appears to be justified. In addition, the value of f_1 seems to decrease with increasing amounts of CH_3CN and the value of $\Delta\varepsilon_1''$ doubles in going from molar ratio $R = [CH_3CN]/[18C6] = 1$ to $R = 4$. Both these trends can be taken as an indication of the interaction between 18C6 and CH_3CN increasing $\Delta\varepsilon_1''$ through an increase of the apparent dipole moment of 18C6 and increasing the dielectric relaxation time of 18C6, $\tau_1 (= 2\pi f_1)^{-1}$, by increasing its moment of inertia.

We recall the Böttcher equation [7] correlating the concentration C of a dipolar species of apparent dipole moment μ to the relaxation strength $\Delta\varepsilon = \varepsilon_0 - \varepsilon_{\infty 1}$ for

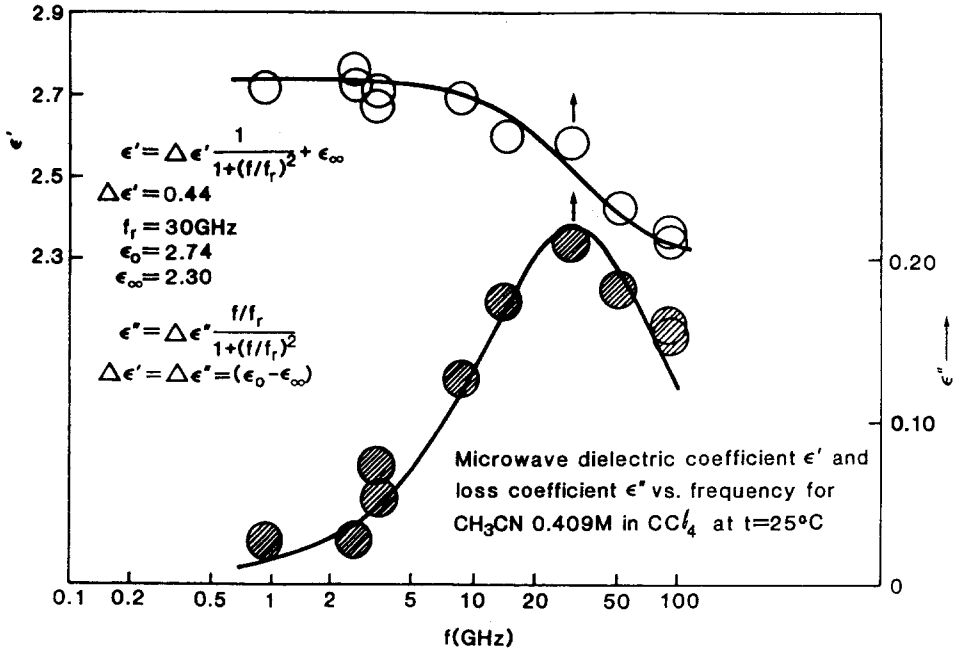

Fig. 2. Microwave dielectric coefficients ε' vs. f and ε'' vs. f for CH_3CN 0.41M in CCl_4 at 25°C.

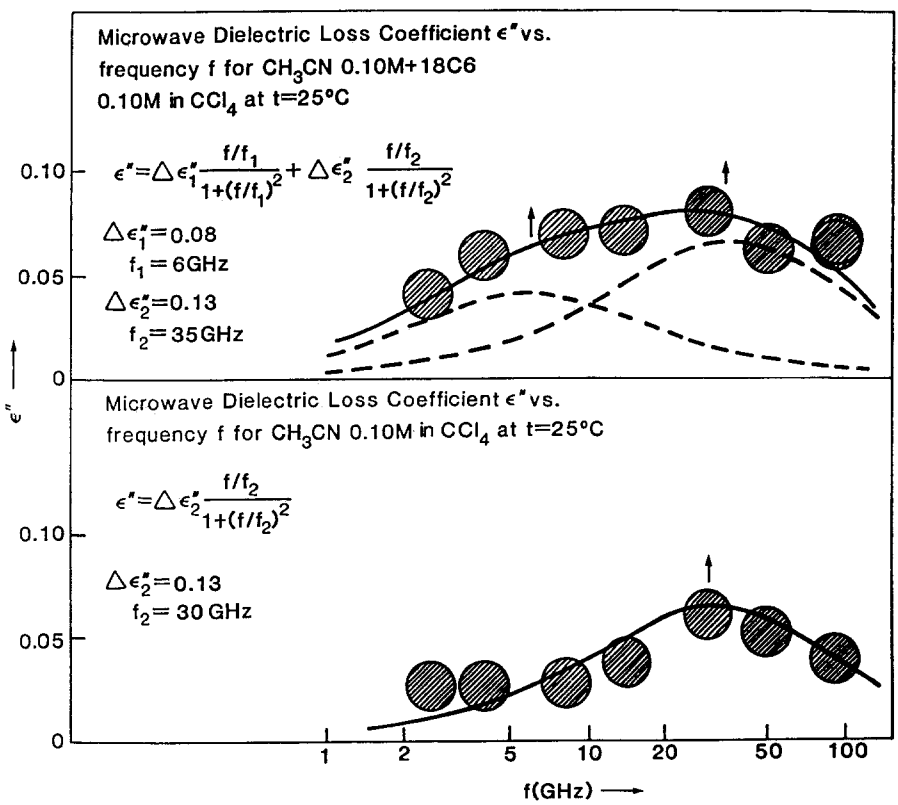

Fig. 3. Microwave loss coefficient ε'' vs. frequency f for the mixture CH_3CN 0.1M + 18C6 0.1M in CCl_4 at 25°C. Microwave loss coefficient ε'' vs. frequency f for CH_3CN 0.1M in CCl_4 at 25°C.

that species

$$\varepsilon_0 - \varepsilon_{\infty 1} = \frac{4\pi L \times 10^{-3}}{(1-\alpha f)^2} \frac{\mu^2}{3kT} \frac{3\varepsilon_0}{2\varepsilon_0 + 1} C \tag{2}$$

where L is Avogadro's number, α is the polarizability and f is the reaction field factor [7]. This can be rewritten, neglecting the polarizability α reacting field f factor term $(1-\alpha f)^2 = 0.9$ with respect to one, as

$$\phi(\varepsilon) = (\varepsilon_0 - \varepsilon_{\infty 1}) \frac{2\varepsilon_0 + 1}{3\varepsilon_0} = \frac{4\pi L \times 10^{-3}}{3kT} \mu^2 C \tag{3}$$

Thus the slope $\mathrm{d}\phi(\varepsilon)/\mathrm{d}C$ should increase with μ^2 for a given species.

Figure 4 shows a plot of $\phi(\varepsilon)$ vs. the molar ratio $R = [CH_3CN]/[18C6]$ for the system $CH_3CN + 18C6$ in CCl_4 at 25°C. The concentration of 18C6 is $C^0_{18C6} = 0.10M$, whereas the concentration of acetonitrile $C^0_{CH_3CN}$ varies from 0.1 to 0.5M. The plot has a positive slope indicating that the apparent dipole moment of 18C6 increases with R (as is also apparent by comparing the $\Delta\varepsilon''_1$ difference of Figures 1 and 3). These results reinforce the notion that 18C6 interacts with CH_3CN, affecting the rotational relaxation parameter of the species involved in the lower frequency relaxation process.

Table I reports all the dielectric parameters ε_0, $\varepsilon_{\infty 1}$, $\varepsilon_{\infty 2}$, f_1 and f_2 used to fit the dielectric spectra of the various R values investigated for the system $18C6 + CH_3CN$ in CCl_4 at 25°C.

Before leaving this system, consider Figure 5, which is a Böttcher plot of $\phi(\varepsilon)$ vs. $C^0_{CH_3CN}$ for acetonitrile alone dissolved in CCl_4. A curvature of the plot is clearly visible which indicates that some of the solvent exists in an apolar form. In fact,

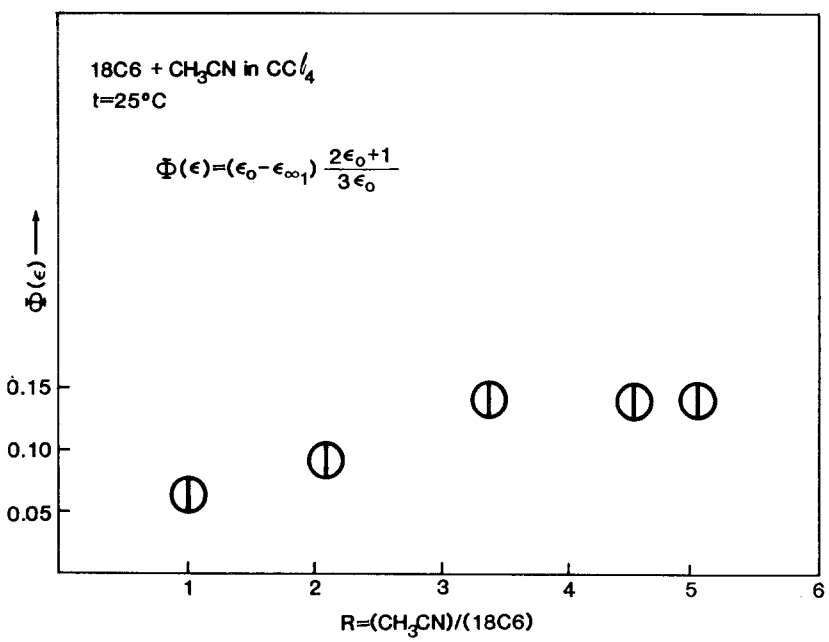

Fig. 4. Böttcher plot of $\phi(\varepsilon) = (\varepsilon_0 - \varepsilon_{\infty 1})(2\varepsilon_0 + 1)/(3\varepsilon_0)$ vs. the molar ratio $R = [CH_3CN]/[18C6]$ for the system $CH_3CN + 18C6$ in CCl_4 at 25°C.

Table I. Collected dielectric parameters $\varepsilon_0, \varepsilon_{\infty 1}, \varepsilon_{\infty 2}, f_1$ and f_2 used to interpret the dielectric spectra of the investigated systems CH_3CN and CH_3CN + macrocycles in CCl_4.[a]

C(M) CH_3CN	ε_0	$\varepsilon_{\infty 1}$	$\varepsilon_{\infty 2}$	f_1(GHz)	f_2(GHz)
0.100	2.37	2.24			30
0.200	2.51	2.24			30
0.303	2.64	2.28			30
0.409	2.74	2.30			30
0.503	2.85	2.30			30
18C6					
0.100	2.32	2.23		7	
18C6 + CH_3CN					
0.100 + 0.100	2.42	2.34	2.21	6	35
0.100 + 0.208	2.61	2.49_5	2.27_2	5	35
0.120 + 0.404	2.85	2.67	2.30	5	35
0.100 + 0.453	2.90	2.72	2.32	5	35
0.100 + 0.504	2.97	2.79	2.32	5	35
15C5					
0.100	2.29	2.22		9	
0.200	2.45	2.26		9	
0.300	2.61	2.26		8	
0.404	2.74	2.30		8	
0.501	2.85	2.30		8	
15C5 + CH_3CN					
0.100 + 0.100	2.53	2.43	2.25	4	30
0.200 + 0.202	2.78	2.60	2.28	4	30
0.301 + 0.301	3.01	2.72	2.28	4	25
0.406 + 0.404	3.35	2.95	2.40	3.8	23
0.501 + 0.499	3.62	3.08	2.40	4.3	23
0.106 + 0.539	3.06	2.87	2.35	5	30

[a] Concentrations are reported with three digits in order to avoid round-off errors in recalculations by others. The values of $\varepsilon_0, \varepsilon_{\infty 1}$ and $\varepsilon_{\infty 2}$ are affected by an average error of $\pm 1\%$; the values of f_1 and f_2 by an average error of $\pm 5\%$.

application of the dimerization equilibrium

$$2CH_3CN \rightleftharpoons (CH_3CN)_2$$

$$2M \rightleftharpoons D \quad \text{with} \tag{4}$$

$$K_d = \frac{[D]}{[M]^2} \quad \text{and} \quad C_0 = [M] + 2[D]$$

leads to the relation: $[M] = (-1 + \sqrt{1 + 8K_d C_0})/4K_d$.

Figure 5 presents the function $\phi(\varepsilon)$ vs. [M] using the minimum value of K_d that linearizes the plot [8] namely $K_d = 0.3_5$. This number is correct only to an order of magnitude, given the relative insensitivity of the linearization of the plot [8]. It is significant, however, that $K_d = 0.3_5$ is within the range of the standard error of the

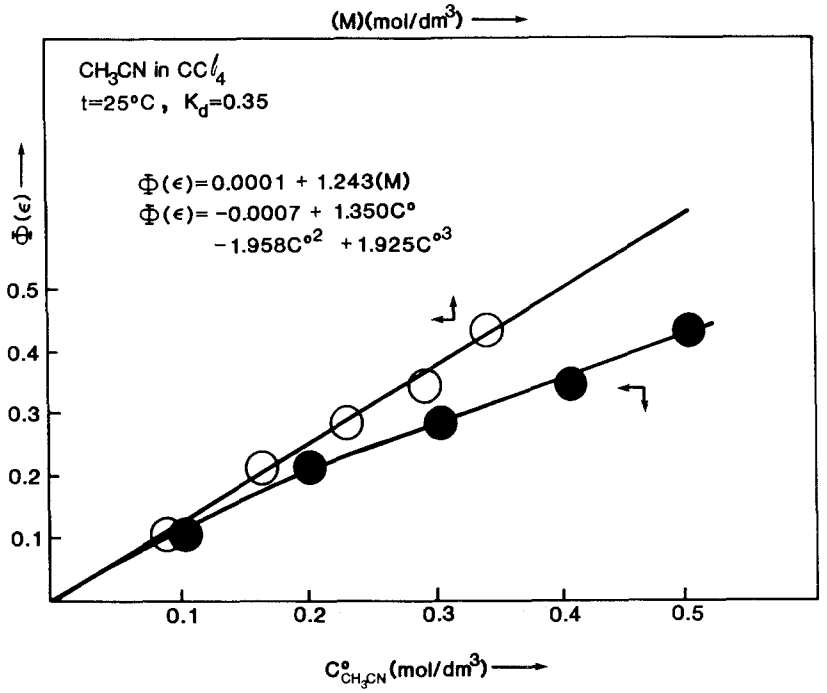

Fig. 5. Böttcher plot (dark circles) of $\phi(\varepsilon)$ vs. the total concentration of acetonitrile $C^0_{CH_3CN}$ for CH_3CN in CCl_4 at 25°C. The solid line corresponds to nonlinear regression giving 50% statistical weight to the origin. Same plot (open circles) of $\phi(\varepsilon)$ vs. the concentration of monomer CH_3CN (M), using a dimerization constant $K_d = 0.35$. The solid line corresponds to linear regression giving 50% statistical weight to the origin.

value $K_d = 0.5_6 \pm 0.2_7$ obtained by Popov by NMR techniques [4] for the dimerization of CH_3CN in CCl_4.

Equation 3 has been used successfully in a comparable concentration range for relatively strongly interactive systems such as dipolar ion-pairs in solution [8]. The correspondence with the K_d obtained by the NMR techniques [4] lends credence to the interpretation of the curvature of Figure 5 as due to dimerization of acetonitrile. The authors believe that the present interpretation based on the results of a relatively modern method such as NMR and a molecular interpretation (Equation 4) advantageously replaces previous 'pre-NMR' phenomenological relations based on the Kirkwood aggregation parameter g.

We were also interested in the possible interaction of another macrocycle, 15C5, with acetonitrile. Although the formation of weak adducts between 18C6 and CH_3CN in the solid state is well known, no quantitative information, to our knowledge, has been reported for 15C5 interacting with CH_3CN in an inert solvent. An inherent experimental advantage is the solubility of 15C5 in CCl_4 that is not limited to ~ 0.1M as in the case of 18C6.

Figure 6 shows a representative plot of ε'' vs. frequency for 15C5 0.4M + CH_3CN 0.4M (in molar ratio $R = 1$) in CCl_4 superimposed on the same plot of 15C5 0.4M alone in CCl_4 at 25°C. The solid lines interpret the loss data by two and one Debye

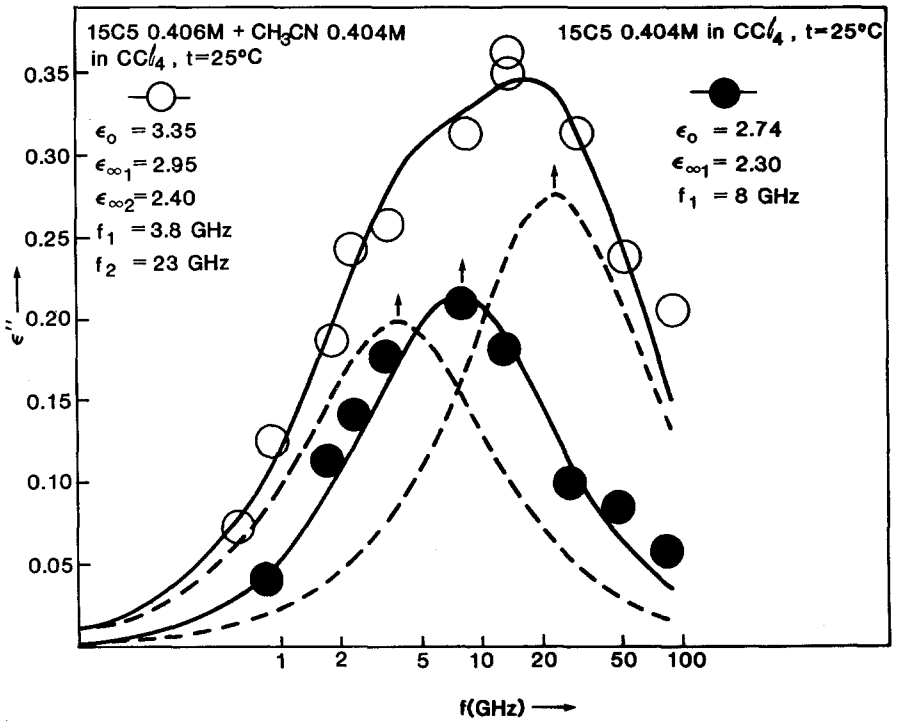

Fig. 6. Representative plot of ε'' vs. frequency f for CH_3CN 0.4M + 15C5 0.4M, at $R = 1$, (open circles) and of 15C5 0.4M in CCl_4 at 25°C (dark circles).

relaxation processes, respectively. While the lower frequency relaxation process drops considerably upon addition of CH_3CN to 15C5, the relaxation stength $\Delta\varepsilon''$ does not change appreciably. This is also shown in Figures 7A and 7B where the Böttcher function $\phi(\varepsilon)$ is plotted against the concentration of 15-crown-5, C^0_{15C5}. Linear regression, assigning 50% statistical weight to the intercept set equal to zero, gives for 15C5 alone

$$r^2 = 0.994, \quad \text{Intercept } -0.0045, \quad \text{Slope} = 0.87 \pm 0.07$$

and for 15C5 + CH_3CN

$$r^2 = 0.996, \quad \text{Intercept } -0.0022, \quad \text{Slope} = 0.79 \pm 0.05$$

The two slopes are the same within experimental error and so are the two apparent dipole moments $\mu_1 = (3.7_7 \pm 0.1_6) \times 10^{-18}$ esu cm and $\mu_1 = (3.5_9 \pm 0.1_2) \times 10^{-18}$ esu cm for the two systems.

These results indicate that at molar ratio $R = 1$, CH_3CN solvates 15C5 as reflected by the lower relaxation frequency f_1, indicating a bulkier rotating entity when 15C5 is present. (This is true whether one retains for the relaxation time of the 15C5 moiety $\tau_1 = (2\pi f_1)^{-1}$, the decay of the polarization, or the microscopic relaxation time denoted τ_{1m}. The two quantities are related and, in the opinion of some [9], $\tau_1 \approx \tau_{1m}$.)

On the other hand, the interaction between 15C5 and CH_3CN at molar ratio $R = 1$ does not seem strong enough to alter the apparent dipole moment μ_1, namely

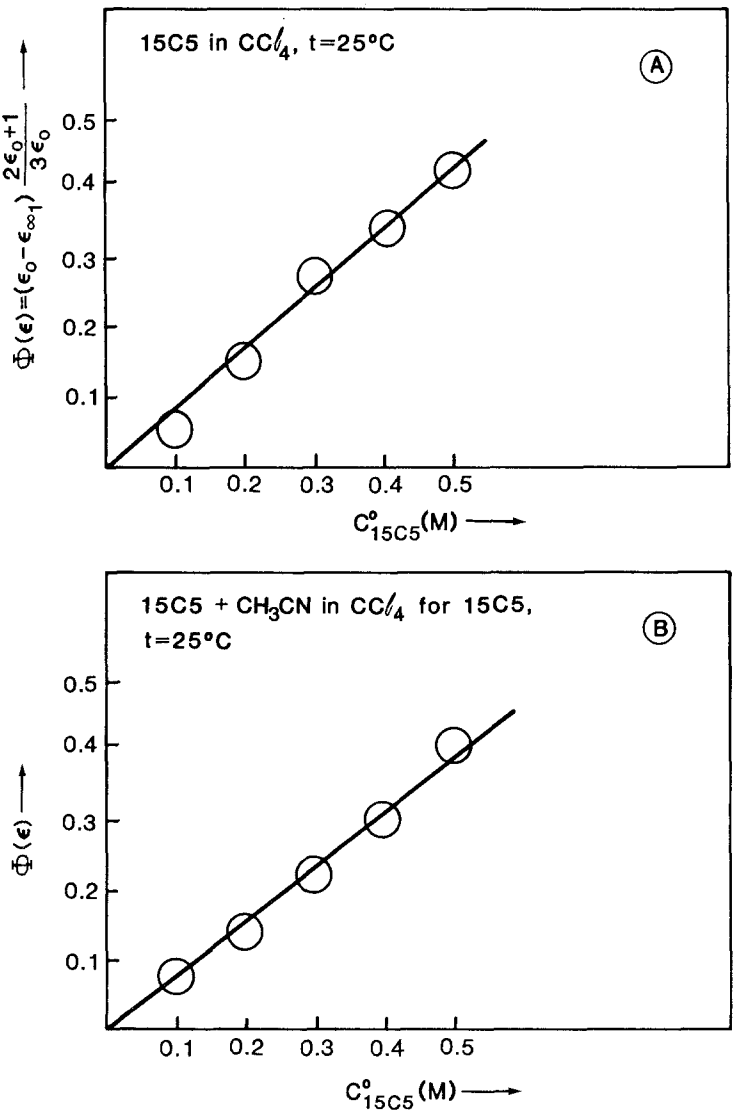

Fig. 7. (A) Böttcher plot for the system 15C5 in CCl_4 of $\phi(\varepsilon)$ vs. the concentration of 15C5, C^0_{15C5} at 25°C. (B) Böttcher plot for the systems CH_3CN + 15C5 at $R = 1$ of $\phi(\varepsilon)$ vs. the concentration of 15C5, C^0_{15C5}, at 25°C.

the formal charge separation or average molecular configuration of 15C5 as shown above. Table I reports all the dielectric parameters used to interpret the dielectric spectra of 15C5 + CH_3CN at molar ratio $R = 1$ and 25°C in CCl_4.

3.2. INFRARED SPECTRA

Figure 8A is the digitized spectrum corresponding to the ν_2 band of CH_3CN in CCl_4. The spectrum, taken relative to a matched cell filled with CCl_4, can be

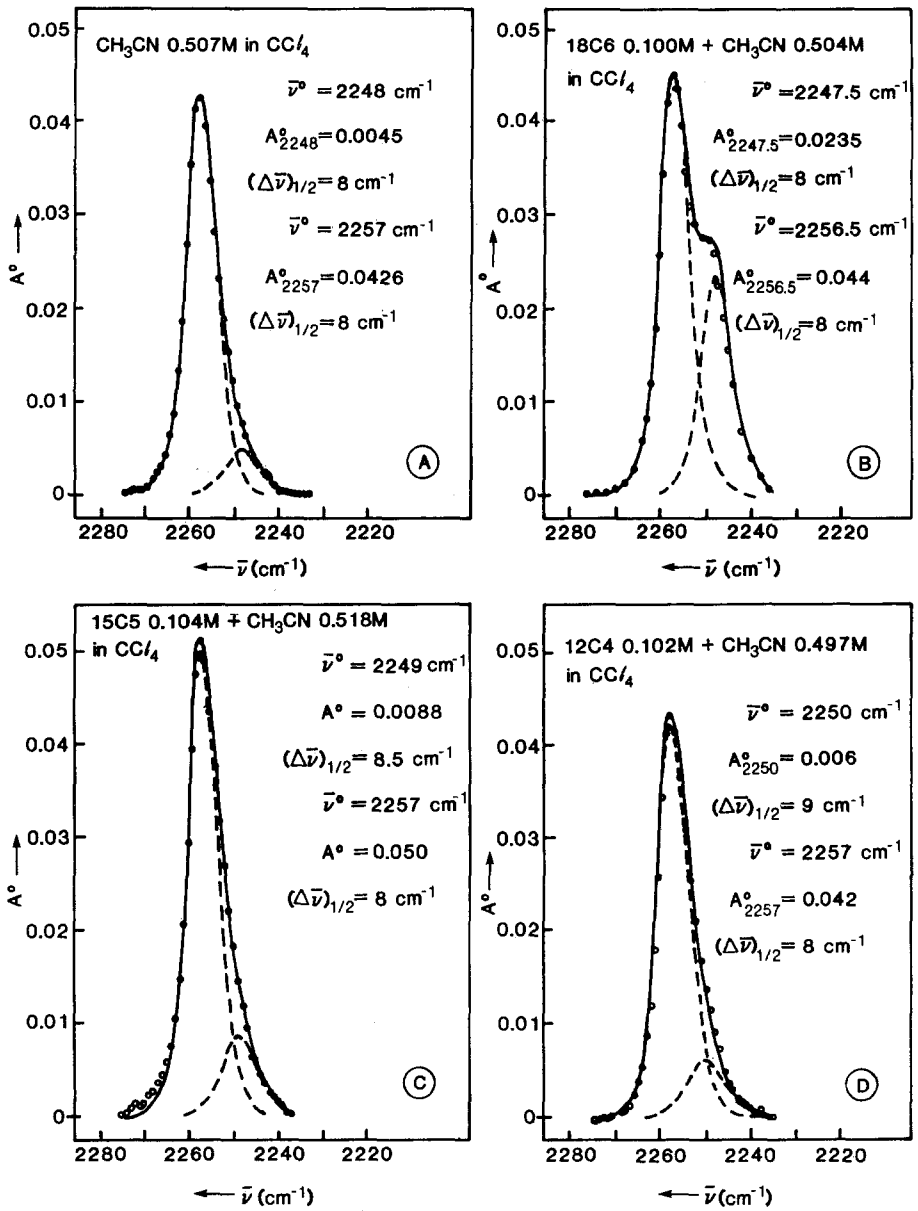

Fig. 8. (A) Representative digitized infrared spectrum of the ν_2 band of CH_3CN 0.5M in CCl_4. The spectral envelope can be deconvoluted into two Gaussian–Lorentzian components. (B) ν_2 band of CH_3CN for the system CH_3CN 0.5M + 18C6 0.1M in CCl_4. (C) ν_2 band of CH_3CN for the system 0.5M + 15C5 0.1M in CCl_4. (D) ν_2 band of CH_3CN for the system CH_3CN 0.5M + 12C4 0.1M in CCl_4.

deconvoluted into two Gaussian–Lorentzian product functions [10]

$$A = \sum_{j=1}^{2} A_j^0 \left[\exp\left(-\frac{(\bar{\nu} - \bar{\nu}_j^0)^2}{2\sigma_j^2} \right) \right] \left[1 + \frac{(\bar{\nu} - \bar{\nu}_j^0)^2}{\sigma_j^2} \right]^{-1} \tag{5}$$

(with σ_j^0 the variance) centered at the wavenumbers $\bar{\nu}_{2255}^0 = 2255\ \mathrm{cm}^{-1}$ and $\bar{\nu}_{2248}^0 = 2248\ \mathrm{cm}^{-1}$. A_j^0 and $(\Delta\bar{\nu}_j)_{1/2}$ are, respectively, the maximum absorbances at $\bar{\nu}_j^0$, and the widths of the band at half maximum absorbance $(A_j^0/2)$.

Figures 8B, 8C and 8D are the digitized infrared envelopes related to the CN-stretch of acetronitrile in the mixtures 0.5M CH_3CN + 0.1M macrocycle (at $R = 5$). These spectral envelopes can also be interpreted by two Gaussian–Lorentzian bands centered at about the same wavenumbers as for CH_3CN in CCl_4. However, the maximum absorbances of the satellite band have increased relative to the one for CH_3CN alone in CCl_4 with the relative sequence A_{2248}^0 (18C6) > A_{2248}^0(15C5) > A_{2248}^0(12C4) > $A_{2248}^0(CCl_4)$.

Figure 9A reports the quantities $A_{2248/l}^0$, namely the normalized maximum absorbance per unit optical path length vs. the molar ratio R for the three macrocycles investigated in CCl_4. Figure 9B presents the same quantities vs. the concentration $C_{CH_3CN}^0$. In this way even the data without added macrocycle can be viewed for comparison. Again it appears that the normalized maximum absorbance of the satellite band at $\bar{\nu}^0 = 2248\ \mathrm{cm}^{-1}$ follows the trend 18C6 > 15C5 > 12C4 > CCl_4.

Raman studies of solutions of acetonitrile in CCl_4 have shown [11] that the deconvolution of the $\bar{\nu}_2$ band of CH_3CN is difficult because of interference attributed to hot bands [11], which occur at the low frequency side of the $\bar{\nu}_2$ band. Attribution of the $2248\ \mathrm{cm}^{-1}$ band for CH_3CN in CCl_4 to hot bands does not necessarily explain the nature of the increase in absorbance of the satellite band upon addition of the macrocycle in the order 12C4 < 15C5 < 18C6.

A possible alternate interpretation of the band at $\bar{\nu}^0 = 2248\ \mathrm{cm}^{-1}$ for CH_3CN in CCl_4 could be found by invoking interaction of the protons of the methyl group of acetonitrile with the chlorine atoms of CCl_4. A model envisaging this specific interaction has indeed been proposed [4].

One could also argue that the CN stretching frequency of acetonitrile in CCl_4 added to macrocycles is affected (in the order 12C4 < 15C5 < 18C6) by interaction of the protons of the $-CH_3$ group with the oxygen atoms of the macrocycle [12], and models have been proposed to this end [4].

Perhaps the most convincing evidence of the existence of a specific additional source of the increase of the absorbance of the satellite band attributable to the macrocycles is shown in Figure 10. Here the maximum absorbance ratio $(A_{2248/l}^0)/(A_{2255/l}^0)$ is plotted against the molar ratio R. The absorbance ratio increases up to about $R = 2$ with the absorbance ratio for 18C6 being larger than those for the other two macrocycles. Thus $R \simeq 2$ apparently represents a 'saturation' of the interaction of the macrocycles with acetonitrile corresponding to a relative increase of A_{2248}^0 with respect to A_{2255}^0. It then follows that, after this 'saturation' occurs, further addition of acetonitrile does not affect the ratio of the absorbances, the individual values of the two bands increasing in the same order with respect to each other as in CH_3CN *alone* in CCl_4. Notice that a similar 'saturation' of the Böttcher dielectric function $\phi(\varepsilon)$ for $R > 3$ is visible in Figure 4.

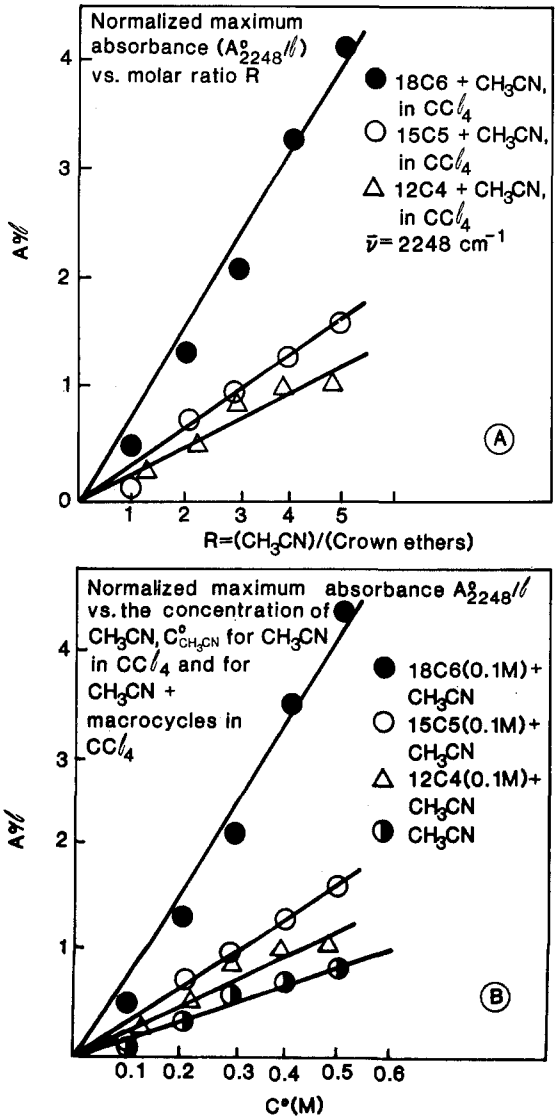

Fig. 9. (A) Normalized maximum absorbance A^0_{2248}/l per unit cell length vs. molar ratio R for the systems CH_3CN + macrocycles investigated in CCl_4 at 25°C. (B) Normalized maximum absorbance A^0_{2248}/l vs. the concentration of acetonitrile, $C^0_{CH_3CN}$, for CH_3CN in CCl_4 and for CH_3CN + macrocycles in CCl_4 at 25°C.

Table II reports all the infrared parameters A^0_j, $\bar{\nu}^0_j$, $(\Delta\bar{\nu}_j)_{1/2}$ of the Gaussian–Lorentzian bands used to interpret the infrared spectra of all the systems investigated.

Table III reports the numerical coefficients of the fitted equations related to the quantities A_0/l vs. either R or C_{CH3CN} for the mixtures shown in Figures 9A and 9B.

Table II. Collected infrared parameters $\bar{\nu}_j^0$, A_j^0, $(\Delta\bar{\nu}_j)_{1/2}$ for the Gaussian Lorentzian product functions used to deconvolute the spectral envelopes, related to the "CN stretch", for the systems CH_3CN and CH_3CN + Macrocycles in CCl_4.[a]

C(M) CH_3CN	$\bar{\nu}^0_{2257}$	A^0_{2257}	$(\Delta\bar{\nu}_{2257})_{1/2}$	$\bar{\nu}^0_{2248}$	A^0_{2248}	$(\Delta\bar{\nu}_{2248})_{1/2}$	l (cm)
0.100	2257.8	0.0217	7.3	2248	0.0017	8.0	0.0199
0.207	2257.5	0.0410	8.0	2248	0.0070	8.0	0.0217
0.302	2257.5	0.0177	8.0	2248	0.0030	8.0	0.00537
0.402	2257.2	0.0320	8.0	2248	0.0037	8.0	0.00544
0.507	2257.0	0.0426	8.0	2248	0.0045	8.0	0.00553
18C6 + CH_3CN							
0.100 + 0.100	2256.7	0.0260	8.5	2248	0.0100	8.0	0.01981
0.100 + 0.201	2257.0	0.0140	8.3	2248.2	0.075	8.0	0.00560
0.100 + 0.302	2256.8	0.0224	8.3	2248.5	0.0116	7.8	0.00556
0.100 + 0.407	2256.5	0.0333	8.0	2247.5	0.0180	7.8	0.00554
0.100 + 0.504	2256.5	0.0440	8.0	2247.5	0.0235	8.0	0.00567
15C5 + CH_3CN							
0.108 + 0.108	2256.6	0.0063	11	2248	0.00075	8.5	0.00557
0.109 + 0.229	2257	0.0163	8	2248.8	0.0040	8.5	0.00549
0.108 + 0.317	2257	0.0292	8	2248.5	0.0055	8.5	0.00551
0.103 + 0.410	2257	0.038	8	2248.5	0.0070	8.5	0.00538
0.104 + 0.518	2256.8	0.050	8	2248.8	0.0088	8.5	0.00545
12C4 + CH_3CN							
0.0976 + 0.119	2257.2	0.0078	7	2250	0.0014	9	0.00547
0.101 + 0.225	2257.1	0.0155	7	2250	0.0027	9	0.00542
0.107 + 0.325	2257.1	0.0265	7	2250	0.0050	9	0.00573
0.105 + 0.409	2257	0.0360	7	2250	0.0060	9	0.00576
0.102 + 0.497	2256.8	0.0420	8	2250	0.0060	9	0.00569
15C5 + CH_3CN							
0.108 + 0.108	2256.5	0.0063	11	2248	0.00075	8.5	0.00557
0.206 + 0.200	2256.5	0.0148	6.3	2251	0.0028	5.0	0.00546
0.301 + 0.304	2256.5	0.0262	8	2248.9	0.0060	8.0	0.00553
0.416 + 0.400	2256.0	0.0380	8	2248.5	0.0075	8.0	0.00576
0.501 + 0.508	2255.8	0.0480	8	2248	0.0115	8.0	0.00556
12C4 + CH_3CN							
0.502 + 0.497	2256	0.0500	8	2248	0.0070	9	0.00577

The last digit in the concentrations, the decimal figures in the $\bar{\nu}_j^0$ values and in the $(\Delta\bar{\nu}_j)_{1/2}$ values and the last digit in the A_j^0 values are affected by a significant error. These digits are reported here in order to avoid round-off errors in recalculations by others.

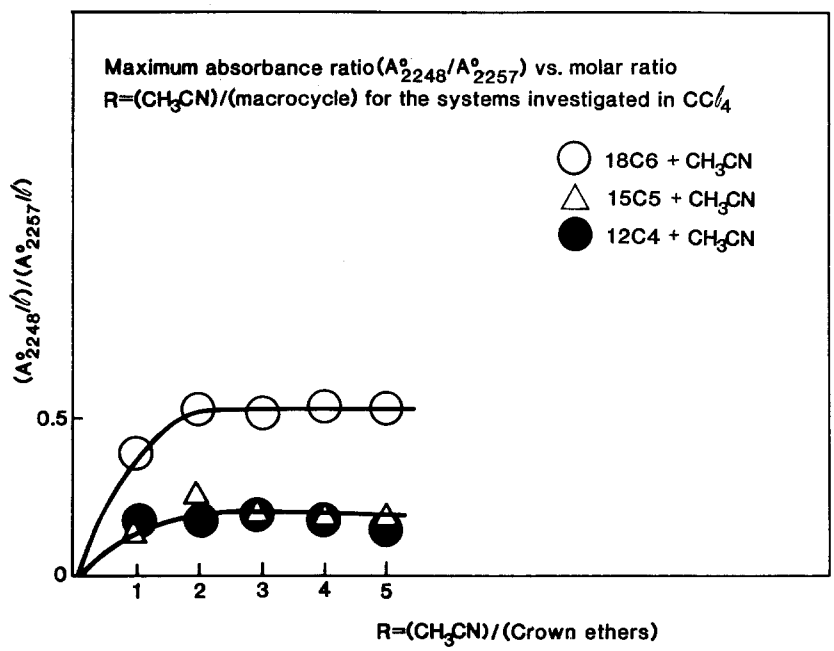

Fig. 10. Maximum absorbance ratio $(A^0_{2248}/l)/(A^0_{2251}/l)$ vs. molar ratio $R = [CH_3CN]/[\text{macrocycle}]$ for the systems investigated in CCl_4. The concentration of macrocycle is fixed at ~ 0.1M.

Table III. Fitted (A^0/l) values for the band at $\bar{\nu}^0 = 2248\ \text{cm}^{-1}$ vs molar ratio R and vs acetonitrile concentration for the macrocycles + acetonitrile mixtures investigated.

	$A^0/l = a + bR$			$A^0/l = \alpha + \beta R + \gamma R^2 + \delta R^3$				
$R = \frac{[CH_3CN]}{[18C6]}$	a	b	r^2	α	β	γ	δ	r^2
18C6 + CH_3CN	−0.0742	0.7969	0.990	−0.0003	0.3973	0.1394	−0.0108	0.999
15C5 + CH_3CN	−0.0185	0.3306	0.989					
12C4 + CH_3CN	0.0027	0.2422	0.975					

	$A^0/l = a + bc$		
	a	b	r^2
CH_3CN	−0.0082	1.6748	0.989

Acknowledgement

The authors are grateful to the National Science Foundation for generous support through grant # CHE 8822333.

Notes and References

1. G. A. Melson (Ed.): *Coordination Chemistry of Macrocyclic Compounds*, Plenum Press, New York (1979).
2. R. M. Izatt and J. J. Christensen (Eds.): *Progress in Macrocyclic Chemistry*, Vol 2. John Wiley, New York, (1981).
3. G. W. Gokel, L. Echegoyen, M. S. Kim, E. M. Eyring, and S. Petrucci: *Biophys. Chem.* **26**, 225 (1987).
4. P. A. Mosier-Boss and A. I. Popov: *J. Am. Chem. Soc.* **107**, 6168 (1985).
5. H. Farber and S. Petrucci: *Dielectric Microwave Spectrometry* (The Chemical Physics of Solvation, Eds. R. R. Dogonadze, E. Kalman, A. A. Kornyshev and J. Ulstrup), Vol. B. Elsevier, Amsterdam (1986).
6. D. Saar and S. Petrucci: *J. Phys. Chem.* **90**, 3326 (1986).
7. C. F. Böttcher: *Theory of Electrical Polarization*, Elsevier, Amsterdam (1973).
8. M. Delsignore, H. Farber, and S. Petrucci: *J. Phys. Chem.* **89**, 4968 (1985).
9. M. Davies: *Dielectric Dispersion and Absorption and Some Related Studies in Condensed Phases* (Dielectric Properties and Molecular Behaviour, Eds. N. Hill, W. E. Vaughan, A. H. Price, and M. Davies), p. 298. Van Nostrand Reinhould Co., London (1969).
10. For a review of this function see: H. Maaser, M. Xu, P. Hemmes, and S. Petrucci: *J. Phys. Chem.* **91**, 3047 (1987); M. Inoue, M. Xu, and S. Petrucci: *J. Phys. Chem.* **91**, 4628 (1987).
11. J. Yarwood and R. Arndt: *The Study of Intermolecular Interactions in the Liquid Phase using Infrared and Raman Band Shapes and Intensities* (Molecular Association: Including Molecular Complexes, Ed. R. Foster) Vol 2, Chapter 4. Academic Press, New York (1979).
12. In the solid state the 18C6 · 2 CH_3CN complex appears to have the methyl protons of acetonitrile hydrogen-bonded to the ether oxygen atoms of 18C6 (see Ref. 6 in [4] above).